

Article

Dual-Control of Autothermal Thermophilic Aerobic Digestion Using Aeration and Solid Retention Time

Silvano Nájera *, Montserrat Gil-Martínez and Javier Rico-Azagra

Electrical Engineering Department, University of La Rioja, c/San José de Calasanz 31, 26004 Logroño, Spain; montse.gil@unirioja.es (M.G.-M.); javier.rico@unirioja.es (J.R.-A.)

* Correspondence: silvano.najera@unirioja.es; Tel.: +34-941-299-496

Academic Editor: José Manuel Poyatos

Received: 11 March 2017; Accepted: 9 June 2017; Published: 13 June 2017

Abstract: Autothermal thermophilic aerobic digestion (ATAD) is an advanced sewage sludge treatment which allows compliance with increasingly demanding regulations. Concerning sludge pasteurization, a certain average temperature must be assured in the digester during batch treatment. Aeration flow is the variable most manipulated to regulate the digester temperature. Additionally, the manipulation of the batch sludge flow—which is related to the solid-retention-time—is considered to improve temperature regulation despite variations in air and sludge temperatures and the variability of raw sludge organic content. Thus, a dual-input control structure was provided where the aeration and solid-retention-time contributed as faster and slower inputs, respectively. Two controllers intervened, and the set-point for the batch average temperature was chosen to meet the minimum effluent quality established by the US regulations or European recommendations, considering that lower set point temperatures save aeration costs. A set-point for the aeration allowed us to achieve an extra goal, which aimed at either reducing operation costs or increasing production rates. The two feedback controllers were designed following the robust control methodology known as quantitative feedback theory (QFT). Improvements were compared with single-input (aeration-flow) control strategy and open-loop control strategy. Simulations were performed on a benchmark non-linear simulation model for ATAD.

Keywords: Autothermal Thermophilic Aerobic Digestion (ATAD); sludge pasteurization; wastewater treatment (WWT); mid-ranging control; quantitative feedback theory (QFT); process control

1. Introduction

New regulations in the increasingly stringent wastewater treatment sector promote the use of advanced wastewater and sludge treatments. The sludge that is obtained in wastewater treatments is rich in nutrients and organic matter, which makes it reusable as a soil fertilizer [1] after proper processing. Autothermal thermophilic aerobic digestion (ATAD) is a reference technology for sludge stabilization and pasteurization [2,3]. ATAD treatment is based on the aeration of the raw sludge in a closed reactor for a specified retention time. When sludge pasteurization is mandatory, the digester is usually operated in batch-mode (a sequence of feeding-reaction-withdrawal that is repeated batch after batch) to avoid hydraulic shorts and ensure time-temperature conditions. By supplying a suitable amount of air, several biochemical reactions consume the organic matter content in the sludge, which reduces the potential of the sludge to attract disease vectors (insects, rodents, birds, etc.) [4]. Exothermic reactions generate heat, which maintains the reactor temperature at around 55 °C without the need to apply external heat energy. The high temperature during the batch time reduces the pathogen concentration in the sludge [5–7].

The control of the reaction is vital to achieving proper stabilization (vector attraction reduction) and pasteurization (pathogen reduction) levels as per the regulations and recommendations guidelines.

The standards by the US Environmental Protection Agency (USEPA) [4,8] and the EU Commission [9] were considered. Several ATAD control approaches have been proposed in the scientific literature. Breider et al. [10] described an intuitive way to regulate the digester temperature through aeration flow. Kim and Oh [11] developed a control method using fluorescence monitoring of the biological activity to search for aeration savings. Wareham et al. [12] pursued the best stabilization level and considered the oxidation-reduction-potential (ORP) to cut off aeration. Zambrano [13] non-linearly varied the aeration during the batch based on the slope of the temperature evolution, which aimed to obtain maximum organic matter degradation without excessive aeration. With the same objectives, Nájera et al. [14] proposed a feedback control structure whose controller was designed following linear robust control techniques. García et al. [15] compared ATAD as a single treatment with dual ATAD and post-anaerobic digestion, where both layouts looked for a medium level of stabilization. Nájera et al. [16] also considered the treated-sludge quality, the treatment-cost, and the rate of treated-sludge to propose different trade-off control strategies. Since relatively small thermophilic temperatures comply with the pasteurization criteria, pasteurization is a common goal in all ATAD control approaches. The study of this goal is relevant in both the single ATAD and dual configuration; the latter can include a second aerobic or anaerobic stage [17].

To carry out any control strategy, the digester temperature is practically the only robust on-line measurable variable that provides relevant information regarding the digestion status. The regulation of the temperature to a required set-point mostly uses aeration flow, which provides major controllability [10]. In addition, the sludge flow can also be manipulated. In the batch operation, the solid-retention-time is preferred to describe the sludge-flow manipulation and can be achieved by changing either the batch time or the sludge volume treated per batch. Nájera et al. [16] discussed the influence of both control variables (air-flow and solid-retention-time) in the digester temperature, and eventually in the quality of the treated-sludge, in the operation-cost and rate of treated-sludge (production-rate).

The use of multiple manipulated inputs is widely used in process control [18–21]. The involvement of two control variables inside the feedback control structures allows the achievement of two control objectives. In this work, one control objective was temperature regulation to a specified set-point that was conveniently selected to ensure the required sludge quality. The other control objective was the regulation of air-flow to a specified set-point that was selected to achieve different goals. The obvious goal was to save aeration-costs by reducing the aeration set-point. On the other hand, higher aeration set-points for the same digester temperature would reduce the solid-retention-time. Next, a second goal was to increase the production-rate by increasing the aeration set-point. The indirect regulation of the production-rate would be useful to adapt the digester sludge-flow to circumstances upstream or downstream (e.g., possible pre-holding tank level near its limits). As smaller digester temperatures save aeration costs, the temperature set-point was fixed to the minimum value to meet the USEPA (or EU) recommendation for pasteurization [8,9]. The result of low thermophilic digestion temperatures is poor stabilization. Anaerobic digestion [22] would complete the treatment at a second stage. Nevertheless, larger temperature set-points favor sludge stabilization (volatile solids reduction), but do not necessarily assure the regulation [4,8] fulfilment.

From a dynamic point of view, both the aeration-flow and the solid-retention-time cooperate in the digester temperature regulation. This temperature is disturbed by the variability of air and sludge temperatures, or by the variability of the organic content of the inlet sludge, amongst others. Thus, robust controllers were designed based on quantitative feedback theory principles [23]. Their particularities for two-input one-output structures are detailed in Rico-Azagra et al. [24].

An ATAD benchmark simulation model [13,25] was used for the study of the digester behavior, for the validation of the control structure, and for evaluations and comparisons.

The remainder of the paper is organized as follows. Section 2 studies the influence of air-flow and solid-retention-time on the digester temperature, and the control strategies are defined, as is the dual-control structure used to achieve them. Appendix A thoroughly describes the method used to

design the robust controllers. Section 3 evaluates the expected performance of the dual-control where quality, cost, and production indexes are evaluated to show the improvements versus single-control and manual control. In Section 4, the main conclusions are presented.

2. Materials and Methods

2.1. Steady-State Analysis of the ATAD

Current benchmark simulation models (BSMs) [26] were extended to ATAD technology through the benchmark simulation model AT_BSM [13,25]. This was used in this work for the ATAD analysis, and for the simulation and validation of the proposed control strategies.

In AT_BSM, the digester (Figure 1a) was modeled as a tank with two completely-stirred volumes (liquid and gaseous phases). Biological reactions and energy balances were considered [27]. The biochemical model (Figure 1b) was based on the standard ASM1 with slight modifications to make it consistent with observations from the ATAD reactors (acid-base reactions and liquid-gas transfers). Temperature evolution was obtained through the system energy balance, which considered several heat fluxes involved in the process: influent and effluent heat energy, heat fluxes through walls and gas-liquid surface, and heat transfer from the mixing equipment. A total number of 24 dynamic variables were included in a state-space model [13]. A 24 h (1 day) cycle sequence was established in AT_BSM: 0.5 h for sewage feeding; 23 h for reaction (aerated reaction phase); and 0.5 h for sludge withdrawal. During each cycle (batch), a portion of the total reactor volume ($V_{ATAD} = 2350 \text{ m}^3$) was drained and filled. Next, the solids retention time (SRT) is given by:

$$SRT = \frac{V_{ATAD}}{Q_{raw}} \tag{1}$$

where Q_{raw} is the mean influent flow per batch. The mean effluent flow per batch Q_{out} is equal to Q_{raw} minus the evaporation shrinkages. For a stable operation of the digester, SRT can be moved over 10–15 d (day). The ability to change SRT involves the existence of a pre-holding tank [13] to regulate the influent flow and to absorb fluctuations of the outlet flow. The influent definition consists of: (i) a constant composition given by simulations of the benchmark simulation model No.2 (BSM2) evaluated by Vrecko et al. [28]; and (ii) a significant variability of the biodegradable content. Departing from an exhaustive analysis of the raw sludge in the BSM2, 2/3 parts of the mixed raw sludge were due to the slowly biodegradable substrate ($X_{s,in}$) [13]. For simplicity, $X_{s,in}$ was used as the principal indicator to quantify the biodegradable organic matter content in the raw sludge. The sludge temperature T_{sludge} and the air temperature T_{air} considered long-term and short-term variations [13]. The mean aeration flow per batch Q_a was rated up to $65,000 \text{ m}^3/\text{d}$.

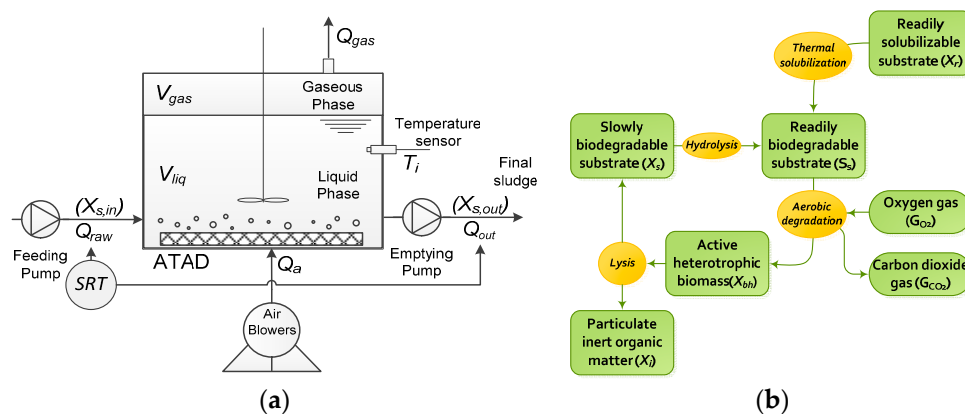


Figure 1. Autothermal thermophilic aerobic digestion (ATAD) (a) Scheme of the process and variables; and (b) Main biochemical reactions. SRT: solids retention time.

Regulation tasks on AT_BSM were performed on the batch average temperature T_{avg} . Manipulated variables SRT and Q_a remained constant for the 1-day batch time, and were updated by the control law batch after batch. Therefore, constant manipulated inputs were considered for the present steady-state analysis. T_{avg} was on-line computed as the mean value of $N_i = 1440$ records of instantaneous temperature T_i . These were captured during the 1-day treatment evolution (one T_i sample was taken every minute). For proper pasteurization, the USEPA [8] establishes a minimum time D (d) as a function of the sludge temperature T_i ($^{\circ}\text{C}$), which is expressed by:

$$D = \frac{50,070,000}{10^{0.14 T_i}} \tag{2}$$

In contrast, the European Commission [9] recommends that the temperature inside the reactor should be over $55\text{ }^{\circ}\text{C}$ for at least 20 h without admixture or withdrawal during treatment. Fuchs and Fuchs [29] asserted that sufficient batch-time at a temperature between 50 and $70\text{ }^{\circ}\text{C}$ assured reliable disinfection. After several simulations on AT_BSM, we adopted T_{avg} set-points around $55\text{ }^{\circ}\text{C}$ to meet the pasteurization regulations.

As in Nájera et al. [16], our analysis studied the steady-state temperature T_{avg} reached after 50 days at constant conditions of manipulated inputs, air and sludge temperatures, and influent composition. Figure 2 shows the results around the temperature of interest $T_{avg} = 55\text{ }^{\circ}\text{C}$. A wide range of manipulated inputs, Q_a and SRT , were analyzed. A relatively high organic matter content $X_{s,in}$ was fixed to 30 kg/m^3 in the analysis so that the required temperature could be provided by the manipulation of both Q_a and SRT over their respective ranges. Considering that Q_a is directly proportional to the aeration cost and SRT is inversely proportional to the sludge flow (production-rate), operating points of “minimum cost” and “maximum production” are highlighted in Figure 2 (some curves have been excluded in Figure 2b since their SRT values were out of the range over 10–15 d).

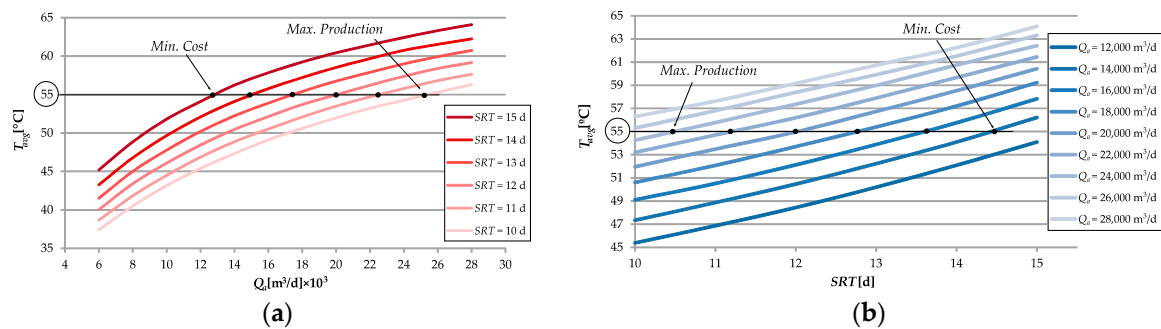


Figure 2. (a) T_{avg} vs. Q_a for SRT over 10–15 d ($X_{s,in} = 30\text{ kg/m}^3$, $T_{air} = 15\text{ }^{\circ}\text{C}$, and $T_{sludge} = 15\text{ }^{\circ}\text{C}$); and (b) T_{avg} vs. SRT for Q_a over 12,000–28,000 m^3/d ($X_{s,in} = 30\text{ kg/m}^3$, $T_{air} = 15\text{ }^{\circ}\text{C}$, and $T_{sludge} = 15\text{ }^{\circ}\text{C}$).

The ratio Q_a/Q_{raw} represents the aeration cost in a fairer way for analysis. It indicates the amount of air required per unit of treated sludge. Figure 3 evaluates that ratio for several production rates from $157\text{ m}^3/\text{d}$ to $235\text{ m}^3/\text{d}$, which corresponded to the SRT from 15 d to 10 d, respectively, as per Equation (1). The bar diagram (Figure 3) shows the trade-off between reducing the aeration cost and increasing the production-rate. Results are shown for several temperatures. They reveal the importance of achieving the strictly required pasteurization temperature to save aeration costs for the same production rate. Temperature $T_{max,st}$ means that the maximum achievable temperature ($61.4\text{ }^{\circ}\text{C}$, $61.1\text{ }^{\circ}\text{C}$, $60.6\text{ }^{\circ}\text{C}$, $60.45\text{ }^{\circ}\text{C}$, $60.1\text{ }^{\circ}\text{C}$, $59.7\text{ }^{\circ}\text{C}$) for each SRT (from 15 d to 10 d, respectively) and for $X_{s,in} = 20\text{ kg/m}^3$; thus, $T_{max,st}$ involved the best attainable stabilization level, which was different for each SRT and Q_a (see Nájera et al. [16] for further details). The aeration-cost savings were around 30% if pasteurization was solely achieved, and was out of scope for this work if this decision compensated a post-treatment for the required sludge stabilization. $T_{avg} = 55\text{ }^{\circ}\text{C}$ and $T_{avg} = 56.8\text{ }^{\circ}\text{C}$ distinguished the minimum required temperature to meet the USEPA and EU pasteurization criteria, respectively.

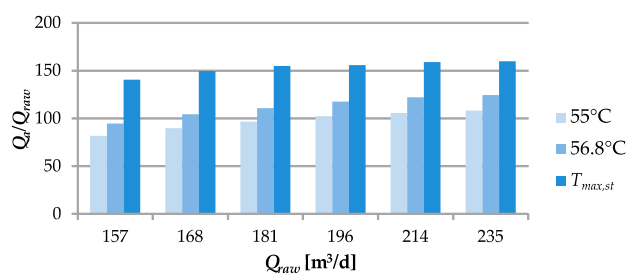


Figure 3. Aeration cost ratio vs. production-rate for several temperatures and $X_{s,in} = 20 \text{ kg/m}^3$.

2.2. Dual-Control System of the ATAD

Two control strategies were attempted to achieve pasteurization temperatures (Table 1): MISO COST, which yielded the lowest aeration cost; and MISO PROD, which yielded the highest production rate. The feedback control structure to accomplish them is shown in Figure 4. One strategy or the other was selected by changing the aeration set-point $Q_{a,ref}$. Overall, smaller values of $Q_{a,ref}$ save aeration costs, but indirectly lead to higher SRT values, which involves lower production rates. On the other hand, higher values of $Q_{a,ref}$ increase the aeration levels to eventually treat more sludge (SRT decreases). Furthermore, $Q_{a,ref}$ can be rated to adapt the effluent flow to a second treatment stage, which, for example, would consist of an anaerobic digestion for full stabilization. For the same digester temperature, shrinkages by evaporation are larger when solid-retention-times are larger. Thus, the strategy that minimizes aeration costs (less Q_a) also minimizes transport costs (less Q_{out}).

Table 1. Control strategies. MISO: multiple input single output.

Quality	Control Strategy		Regulated Variables Inside Feedback Control Structure (Figure 4)	Label
	Aeration Cost	Production Rate		
Strictly pasteurization (Goal)	Higher (Side effect)	Highest (Goal)	USEPA: $T_{avg,ref} = 55 \text{ }^\circ\text{C}$, $Q_{a,ref} = 22,524 \text{ m}^3/\text{d}$ EU: $T_{avg,ref} = 56.8 \text{ }^\circ\text{C}$, $Q_{a,ref} = 26,100 \text{ m}^3/\text{d}$	MISO PROD
	Lowest (Goal)	Lower (Side effect)	USEPA: $T_{avg,ref} = 55 \text{ }^\circ\text{C}$, $Q_{a,ref} = 15,053 \text{ m}^3/\text{d}$ EU: $T_{avg,ref} = 56.8 \text{ }^\circ\text{C}$, $Q_{a,ref} = 17,500 \text{ m}^3/\text{d}$	MISO COST

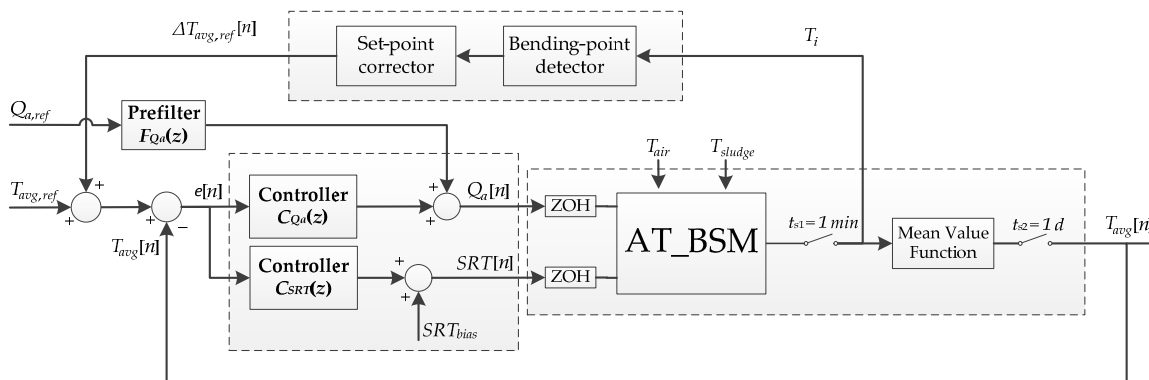


Figure 4. Block diagram of the control structure. ZOH: zero-order-hold.

The feedback control structure assured that the batch average temperature T_{avg} was regulated to a specified set-point $T_{avg,ref}$ despite changes in temperatures T_{air} , T_{sludge} , and variability of the biodegradable organic matter content in the raw sludge $X_{s,in}$. Whenever the pasteurization requirement was met, as small as possible values for $T_{avg,ref}$ were selected, since smaller temperatures reduce aeration costs for the same production rate. Accordingly, the $T_{avg,ref}$ was chosen as $55 \text{ }^\circ\text{C}$ or $56.8 \text{ }^\circ\text{C}$ for USEPA or EU recommendations, respectively (Table 1).

If the input energy that $X_{s,in}$ carried in was not sufficient to maintain the $T_{avg,ref}$, this set-point was reduced for stable operation [14]. This situation was observed through a sharp decrease in the slope of the batch T_i -temperature profile. An algorithm for its detection is described in Zambrano [13] and Zambrano et al. [25]. Here, it was implemented under the block “bending-point detector” of Figure 4. Consequently, Nájera et al. [14] presented a fuzzy logic algorithm to provide the corrections $\Delta T_{avg,ref}$. This task was included in the block “set-point corrector” of Figure 4.

The main novelty in feedback control was the use of two manipulated inputs— Q_a and SRT —to regulate the digester temperature. The fastest input Q_a quickly reacted to any T_{avg} temperature deviation, and progressively gave way to the participation of the slowest input SRT . In this way, Q_a recovered its steady state $Q_{a,ref}$ to meet steady-state control strategies. SRT deviated from its bias point whenever any disturbance persisted. The dynamic collaboration between the two inputs was tailored by a proper design of controllers C_{Q_a} and C_{SRT} based on a robust methodology in Rico-Azagra et al. [24] in the framework of quantitative feedback theory (QFT) with the following main characteristics summarized. Appendix A provides details on the design of the controllers from a more technical point of view for robust control practitioners. The dual-control design first required dynamic modeling of the process. Thus, dynamical models were identified from the two manipulated inputs (SRT, Q_a) to the output (T_{avg}), and from the disturbance inputs (T_{air}, T_{sludge}) to the output (T_{avg}). Several operating points were considered, as summarized in Table 2. This yielded dynamical models with known parameter uncertainty (see Appendix A). A thorough study of the dynamic properties of the process models helped to allocate the frequency band between the two manipulated inputs: Q_a was planned to work at higher frequencies than SRT to achieve a better transient performance. The frequency of 20 rad/s was the frontier between input contributions. The control specifications were guaranteed for the whole set of models. Hence, the terminology of *robust* control is used. For robust stability, a phase margin of 45° was selected. As performance specifications, it was decided that sharp variations in T_{air} and T_{sludge} up to $\pm 5^\circ\text{C}$ between two consecutive batches should not deviate T_{avg} more than $\pm 0.6^\circ\text{C}$ from its set-point $T_{avg,ref}$. Furthermore, this set-point should be recovered at no longer than seven days. Thus, the robust controllers were designed based on the process models and the control specifications (see Appendix A). The controllers were:

$$C_{SRT}(z) = \frac{0.4z^2}{(z-1)(z-0.71)} \quad (3)$$

$$C_{Q_a}(z) = \frac{7274.703(z-0.652)}{z-0.7625} \quad (4)$$

where the variable z is introduced by the Z-transform, which is a method for the design of sampled-data control systems [30]. Here, the sample-time equaled the batch time (i.e., 1 day). In Figure 4, each sample was distinguished by the index n . The “zoh” block performed a zero-order-hold of the computed control actuations during the 1-day treatment. The “mean-value-function” computed T_{avg} each day as the mean value of 1440 records of instantaneous temperature T_i . A T_i sample was taken every minute ($t_{s1} = 1$ min). Additionally, the sampler of the output to update the control law was labelled $t_{s2} = 1$ d.

Table 2. Set of equilibrium points. $T_{air} = T_{sludge} = 15^\circ\text{C}$.

SRT (d)	11	12	13	14
Q_a (m^3/d) ($T_{avg,ref} = 55^\circ\text{C}$)	22,524	20,025	17,426	15,053
Q_a (m^3/d) ($T_{avg,ref} = 56.8^\circ\text{C}$)	26,100	23,000	20,000	17,500

Note: $X_{s,in}$ was considered above $30 \text{ kg}/\text{m}^3$ during the experiments.

A step-change in the Q_a set-point would deviate T_{avg} from its set-point, which would be properly corrected by Equations (3) and (4) in a similar way, as T_{avg} deviations due to step-changes in T_{air} and T_{sludge} were compensated. However, that step-change in Q_a set-point was driven straight away to the

actuation Q_a at the step time. A pre-filter (F_{Q_a} in Figure 4) could conveniently smooth the peak at the beginning of the transient response of Q_a . In our case, a suitable pre-filter was:

$$F_{Q_a}(z) = \frac{0.0239761z^4}{(z - 0.6065)^4} \quad (5)$$

To point out the benefits of using two control inputs, MISO (Multiple Input Single Output) control strategies in Table 1 were compared with SISO (Single Input Single Output) control, which uses a single control input. In this last case, only the aeration flow (Q_a) could provide the T_{avg} regulation capacity required by the control specifications for robust disturbance rejection. Accordingly, the designed controller was:

$$C_{Q_a}^{SISO}(z) = \frac{7079.75z(z - 0.6952)}{(z - 1)(z - 0.1081)} \quad (6)$$

In the SISO strategy, SRT takes a fixed value (i.e., this input does not participate in the closed-loop dynamic regulation). Equation (6) provided the expected closed-loop control specifications for any SRT value in Table 2. An even simpler control method would manually fix both the Q_a and SRT ; thus, they would not participate in the dynamic T_{avg} regulation. We denote this mode as OL (open-loop).

3. Results and Discussion

This section shows several time-domain simulations that were run on the AT_BSM inside the control scheme of Figure 4.

Figure 5 shows the time evolution of the main variables in a first experiment. $X_{s,in}$ remained constant at 30 kg/m^3 , and sudden changes of $\Delta T_{sludge} = -3 \text{ }^\circ\text{C}$ and $\Delta T_{air} = -5 \text{ }^\circ\text{C}$ took place at $t = 50 \text{ d}$ and $t = 70 \text{ d}$, respectively. Maximum deviations of T_{avg} ($0.39 \text{ }^\circ\text{C}$ and $0.27 \text{ }^\circ\text{C}$) were below the maximum permitted of $0.6 \text{ }^\circ\text{C}$ for a $5 \text{ }^\circ\text{C}$ disturbance step, and the settling-time to recover the $55 \text{ }^\circ\text{C}$ set-point was around seven days as expected. In the first moments after any disturbance, Q_a quickly assumed the regulation task, and progressively SRT became more relevant. The steady state of those manipulated inputs was reached before 20 days as prescribed. In steady-state, the SRT necessarily reached different equilibria to compensate the disturbances. However, Q_a always recovered the set-point $Q_{a,ref}$. In this way, $Q_{a,ref}$ was conveniently selected based on the desired strategy: minimum aeration cost (MISO COST) for $t < 90 \text{ d}$, or maximum production rate (MISO PROD) for $t > 90 \text{ d}$. Focusing on the $Q_{a,ref}$ change that took place at $t = 90 \text{ d}$, it could check the expected performance in the T_{avg} set-point recovery and the smooth transition of manipulated inputs SRT and Q_a .

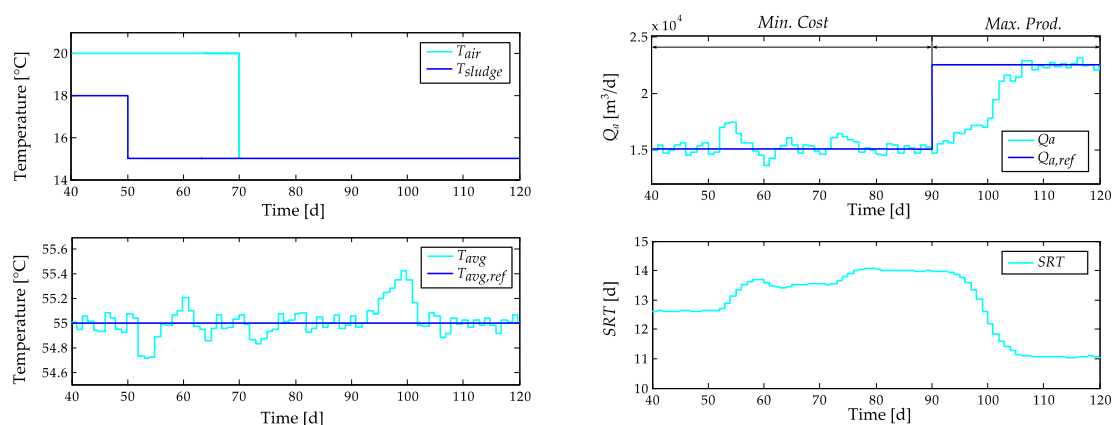


Figure 5. Time domain performance.

A second experiment considered variability in $X_{s,in}$, T_{air} , and T_{sludge} (see Figure 6a). Figure 6b depicts the evolution of the main variables involved in a MISO COST feedback control strategy.

The digester temperature T_{avg} was conveniently regulated to 55 ± 0.2 °C thanks to a fast actuation Q_a (around $Q_{a,ref}$ of minimum cost), which compensated the fastest disturbance dynamics, and to a slow actuation SRT , which mainly compensated the midterm variability of air and sludge temperatures. On the other hand, Figure 7a depicts the evolution of the digester temperature T_{avg} for manual control, where $Q_a = 18,750$ m³/d and $SRT = 12.5$ d. The absence of feedback information impeded a suitable regulation of the temperature, which deviated from the desired value due to the variability of input conditions (Figure 6a). Figure 7b shows the variables for a SISO feedback control strategy where $SRT = 12.5$ d. The digester temperature T_{avg} was conveniently regulated to 55 ± 0.2 °C thanks to the single actuation of Q_a . The absence of a second controller to handle SRT impeded the achievement of a second goal by means of an extra set-point.

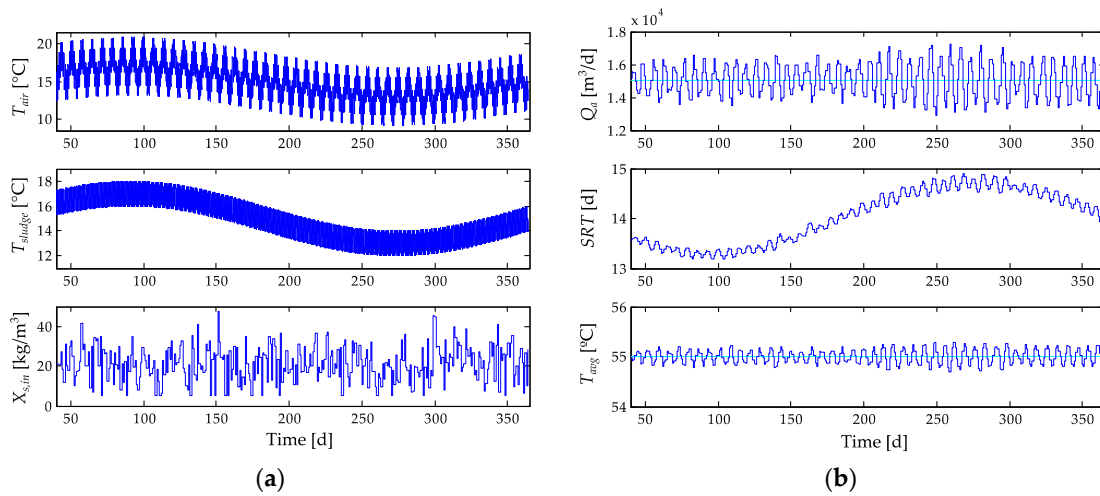


Figure 6. Validation experiment: (a) disturbance inputs; and (b) control variables and controlled variable for MISO COST strategy.

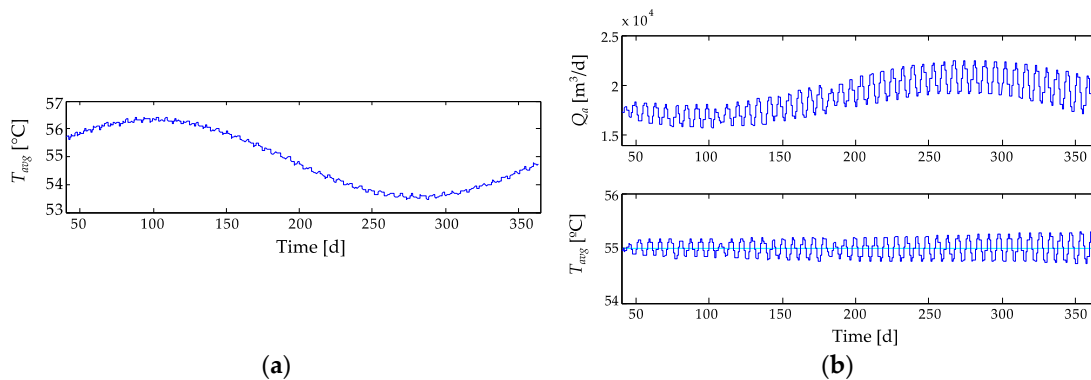


Figure 7. Validation experiment: (a) controlled variable for open-loop (OL) strategy ($SRT = 12.5$ d and $Q_a = 18,750$ m³/d); and (b) control variable and controlled variable for single input single output (SISO) control ($SRT = 12.5$ d).

Finally, considering $X_{s,in}$, T_{air} , and T_{sludge} in Figure 6a, the AT_BSM simulations were separately performed for the comparison of several control strategies. The following evaluation indexes were computed using the data for the same period of 100 d ($N = 100$ batches).

- (i) Pasteurization USEPA Index— $I_{QPUSEPA}$ (%) quantifies the quality of pasteurization as per USEPA guidelines [4,8]:

$$I_{QPUSEPA} = \frac{\sum_{j=1}^N I_{Qpa}^{(j)} Q_{raw}^{(j)} [\text{m}^3 \text{d}^{-1}]}{\sum_{j=1}^N Q_{raw}^{(j)} [\text{m}^3 \text{d}^{-1}]} 100, \quad \text{where} \quad I_{Qpa}^{(j)} = \sum_{i=1}^{N_i} \frac{t_{s1} [\text{d}]}{D^{(i)} [\text{d}]} \quad (7)$$

where $t_{s1} = 6.94 \times 10^{-4}$ d is the sampling time of intra-batch T_i -temperature records, $N_i = 1440$ is the number of T_i -samples in a batch, and $D^{(i)}$ (Equation (2)) is the minimum time required at T_i -temperature. An $I_{QPUSEPA}$ index value equal to 100% meant strict agreement with the regulation. $I_{QPUSEPA}$ greater than 100% was safer, but revealed worthless expenses.

- (ii) Pasteurization EU Index— I_{QPEU} (%) computed the percentage of treated-sludge that met the EU recommendation (55 °C for at least 20 h) [9]:

$$I_{QPEU} = \frac{\sum_{j=1}^N k_{paste}^{(j)} Q_{raw}^{(j)} [\text{m}^3 \text{d}^{-1}]}{\sum_{j=1}^N Q_{raw}^{(j)} [\text{m}^3 \text{d}^{-1}]} 100, \quad \text{where} \quad k_{paste}^{(j)} \begin{cases} 0 & \text{if } PTime^{(j)} < 20 \text{ h} \\ 1 & \text{if } PTime^{(j)} > 20 \text{ h} \end{cases} \quad (8)$$

where $PTime^{(j)}$ (h) represents the total time in which the sludge has been at a temperature greater than 55 °C during the aerated reaction phase of the j -th batch. One hundred percent corresponds to the maximum I_{QPEU} value that was attainable. I_{QPEU} values smaller than 100% indicated that some batch violated the EU regulation.

- (iii) Cost Index— I_C (%) considers the aeration and pumping energies employed per unit of treated sludge volume. The index is normalized as a percentage of an average energy requirement ($E_{ref} = 12$ kWh/m³ sludge) extracted from USEPA [8]:

$$I_C = \frac{E_{Qa} [\text{kWh}] + E_{pump} [\text{kWh}]}{E_{ref} [\text{kWh m}^{-3}] \sum_{j=1}^N Q_{raw}^{(j)} t_{batch} [\text{m}^3]} 100, \quad \text{where} \quad \begin{cases} E_{Qa} = 0.04 \sum_{j=1}^N Q_a^{(j)} t_{batch} \\ E_{pump} = 0.04 \sum_{j=1}^N (Q_{raw}^{(j)} t_{batch} + Q_{out}^{(j)} t_{batch}) \end{cases} \quad (9)$$

where E_{Qa} is the aeration energy; E_{pump} is the pumping energy; and t_{batch} is the batch-time (1 day).

- (iv) Production Index – I_p (%) is expressed as a ratio between the treated sludge flow and the maximum flow that could be treated:

$$I_p = \frac{\sum_{j=1}^N Q_{out}^{(j)} [\text{m}^3 \text{d}^{-1}]}{N \sum_{j=1}^N Q_{rawmax}^{(j)} [\text{m}^3 \text{d}^{-1}]} 100, \quad \text{where} \quad Q_{rawmax} = \frac{V_{ATAD}}{SRT_{min}} \quad (10)$$

I_p is a reliable index only if the ATAD is properly operated (i.e., the pasteurization index should also reach suitable values). For example, an over-flow event in the pre-holding tank or the desire of maximizing the production rate would involve the digester being operated at full-capacity, giving a maximum I_p . However, part of the raw sludge could not be properly treated.

The strategies compared are summarized in Table 3. The desired digester temperature was chosen to meet the minimum level of pasteurization required by the regulation. Thus, either 55 °C or 56.8 °C were chosen to meet the USEPA or EU criteria, respectively. Accordingly, the feedback control strategies adapted their $T_{avg,ref}$. The OL strategy lacked feedback control loops. It used fixed Q_a and SRT , which were estimated off-line. First, a mean $SRT = 12.5$ d was adopted. Then, $Q_a = 18,750$

m^3/d was estimated to achieve $T_{avg} = 55\text{ }^\circ\text{C}$, considering a theoretical behavior (mean temperatures $T_{air} = T_{sludge} = 15\text{ }^\circ\text{C}$ and ideal constant composition of the influent, with $X_{s,in} = 30\text{ kg}/m^3$). Another $Q_a = 21,500\text{ }m^3/d$ was similarly estimated to achieve $T_{avg} = 56.8\text{ }^\circ\text{C}$. The SISO strategy used a feedback control structure, which regulated T_{avg} to $T_{avg,ref}$ by moving Q_a as the feedback controller (Equation (6)) dictates; SRT was manually fixed to 12.5 d. All MISO strategies used the same control structure (Figure 4) and control elements (Equations (3)–(5)). MISO COST and MISO PROD set-points are detailed in Table 1. A standard MISO strategy (MISO STD) selected $Q_{a,ref}$ values in between those of MISO COST and MISO PROD strategies and avoided extreme behaviors since the minimization of aeration costs involves minimum production rates, and the maximization of production rates involves maximum aeration costs.

Table 3. Strategies for comparisons.

	OL	SISO	MISO STD	MISO COST	MISO PROD
Q_a (m^3/d)	18,750 (USEPA) 21,500 (EU)	Free feedback regulated	Feedback regulated to $Q_{a,ref} = 18,750$ (USEPA) or to $Q_{a,ref} = 21,500$ (EU)	Feedback regulated to $Q_{a,ref}$ in Table 1	Feedback regulated to $Q_{a,ref}$ in Table 1
SRT (d)	12.5	12.5	Free feedback regulated	Free feedback regulated	Free feedback regulated

The evaluation indexes are presented in Table 4. Since the set-point temperature was chosen to strictly meet either the USEPA or EU regulations, the yielded quality indexes fully agreed with it. They revealed how a less-detailed criterion (EU regulation) led to safer quality levels, but involved higher cost indexes. For the following comparisons, let us take as the meaningful quality index $I_{QPUSEPA}$ for $T_{avg,ref} = 55\text{ }^\circ\text{C}$ and I_{QPEU} for $T_{avg,ref} = 56.8\text{ }^\circ\text{C}$. Comparing the OL and SISO strategies, both yielded the same I_P since both used the same SRT . A smaller expense I_C for OL involved insufficient aeration, which was in consonance with a poorer quality index. Therefore, closed-loop control was compulsory for continuous supervision and correction of the digester temperature in such a way that the required quality was achieved, and the SISO and MISO control strategies proved this. The added value of MISO vs. SISO strategies is the possibility of attending to a second objective in MISO control. Thus, the MISO COST strategy reduced the aeration expenses (smaller I_C) in comparison with the SISO control to achieve a similar quality. In the same way, the MISO PROD strategy improved the production-rate in comparison with the SISO control (see their I_P). Figure 3 pointed out the trade-off between minimizing the aeration-cost and maximizing the production-rate. Consequently, a smaller I_P in the MISO COST than in the SISO was the price paid for a smaller I_C in the former. A larger I_C in the MISO PROD than in the SISO was the price paid for a larger I_P in the former. Nevertheless, the flexibility of the MISO control ensures that the plant operator has full control of those objectives thanks to a closed-loop that can regulate them. As evidence of this, the MISO STD yielded similar indexes to the SISO control.

Table 4. Evaluation of strategies.

	$T_{avg} = 55\text{ }^\circ\text{C}$ (USEPA)				$T_{avg} = 56.8\text{ }^\circ\text{C}$ (EU)			
	$I_{QPUSEPA}$ (%)	I_{QPEU} (%)	I_C (%)	I_P (%)	$I_{QPUSEPA}$ (%)	I_{QPEU} (%)	I_C (%)	I_P (%)
OL	100.61	7.17	34.28	74.75	175.92	44.9	39.12	74.91
SISO	106.62 (5.97%)	0	35.18 (2.63%)	74.76 (0.01%)	191.32 (8.75%)	100	40.37 (3.20%)	74.96 (0.07%)
MISO STD	106.42 (5.77%)	0	34.83 (1.70%)	73.66 (−1.46%)	190.99 (8.57%)	100	39.89 (1.97%)	73.53 (−1.84%)
MISO COST	105.08 (4.44%)	0	32.32 (−5.72%)	63.93 (−14.47%)	188.55 (7.18%)	100	37.18 (−4.96%)	64.39 (−14.04%)
MISO PROD	107.81 (7.16%)	0	37.04 (8.05%)	82.93 (10.94%)	193.9 (10.22%)	100	42.54 (8.74%)	83.42 (11.36%)

Note: In brackets the indexes are expressed as a percentage of the OL indexes.

4. Conclusions

This paper has shown a novel feedback control structure for ATAD reactors, which takes advantage of the use of air-flow and the solid-retention-time to regulate the digester temperature to a desired set-point. The air-flow supplies a fast reaction against temperature deviations, meanwhile the solid-retention-time dominates the steady-state temperature regulation. Two feedback controllers compute these actuations. This dual control also affords the regulation of the air-flow (the fastest input) to a desired set-point, thanks to which different strategies can be attempted for the same pair of controllers. Obviously, the air-flow set-point has a direct influence on the aeration cost, which can therefore be conveniently handled. Furthermore, the air-flow set-point indirectly conditions the solid-retention-time to achieve the digester temperature. Thus, the air-flow set-point confers a great flexibility to obtain a maximum production-rate, or to conveniently adapt the production-rate to upstream or downstream plant operations. The digester temperature has been regulated to the minimum value that assures USEPA (or EU) recommendations for pasteurization. Similarly, the temperature set-point could be raised, promoting larger stabilization levels, but higher aeration-costs.

Dual-input control strategies were compared with a single-input (aeration) control strategy and a manually controlled reaction. Certain indexes showed the benefits of the novel structure. These indexes evaluated the pasteurization quality (as per USEPA and EU recommendations), the operation cost (aeration, sludge feeding, and sludge withdrawal), and the production-rate.

The feedback controllers were designed in the frequency domain based on the principles of quantitative feedback theory (QFT). The robust controllers assured the temperature regulation based on prescribed closed-loop performance and stability, despite variations of air and sludge temperatures and variations of the raw sludge organic content.

A benchmark simulation model for ATAD technology was used for the preliminary studies, the identification of simple models for control design, the validation experiments, the computation of the evaluation indexes, and for the comparison of control strategies.

Acknowledgments: The authors thank La Rioja Government for the financial support (project IMPULSA 2010/01 and Scholarship PhD program of S. Nájera) of this work.

Author Contributions: S. Nájera and M. Gil-Martínez conceived the idea of ATAD dual control, and all authors conceived the control strategies and discussed the results. S. Nájera performed the ATAD analysis, the control model identification, the validation experiments, the evaluation index definition, and the comparison of different control strategies. J. Rico-Azagra defined the control specifications and designed the QFT robust controllers. S. Nájera wrote the manuscript with the collaboration of M. Gil-Martínez and the approval of J. Rico-Azagra.

Conflicts of Interest: The authors declare no conflict of interest.

Appendix A. Design of MISO Robust Control for ATAD

This section summarizes the methodology used to design the robust control system based on the principles of QFT (quantitative feedback theory). It follows the method in Rico-Azagra et al. [24] for systems that use several manipulated inputs to regulate a single output.

First-order linear dynamical models on the s -Laplace variable [30] can suitably fit the dynamic response of $T_{avg}(t)$ when the reactor inputs— $SRT(t)$, $Q_a(t)$, $T_{air}(t)$, $T_{sludge}(t)$ —experiment step changes from their equilibrium values (Table 2). Tests were performed on the AT_BSM. The set of equilibrium values were chosen in accordance with the steady-state analysis in Section 2.1. Experiment step sizes were: ± 1 d for SRT , ± 1000 m³/d for Q_a , and ± 5 °C for T_{air} and T_{sludge} . Whenever the $X_{s,in}$ composition of the inlet sludge could provide $T_{avg,ref}$, the linear dynamical models were not affected by different $X_{s,in}$. The set of identified plant models can be expressed as first-order transfer-functions whose gain and time-constant can take several values over a certain range:

$$P_{Q_a}(s) = \frac{T_{avg}(s)}{Q_a(s)} = \frac{k_{Q_a}}{(\tau_{Q_a}s + 1)}; \quad k_{Q_a} \in [0.73, 1.5] \times 10^{-3}; \quad \tau_{Q_a} \in [5.93, 9.6] \quad (A1)$$

$$P_{SRT}(s) = \frac{T_{avg}(s)}{SRT(s)} = \frac{k_{SRT}}{(\tau_{SRT}s + 1)}; \quad k_{SRT} \in [1.49, 2.06]; \quad \tau_{SRT} \in [6.59, 9.51] \quad (A2)$$

$$P_{Tair}(s) = \frac{T_{avg}(s)}{T_{air}(s)} = \frac{k_{Tair}}{(\tau_{Tair}s + 1)}; \quad k_{Tair} \in [0.15, 0.23]; \quad \tau_{Tair} \in [6.15, 9.5] \quad (A3)$$

$$P_{Tsludge}(s) = \frac{T_{avg}(s)}{T_{sludge}(s)} = \frac{k_{Tsludge}}{(\tau_{Tsludge}s + 1)}; \quad k_{Tsludge} \in [0.58, 0.59]; \quad \tau_{Tsludge} \in [6.43, 9.61] \quad (A4)$$

Time constants τ_{Qa} , τ_{SRT} , τ_{Tair} and τ_{sludge} are expressed in d. Gain k_{Qa} is expressed in $^{\circ}\text{C}\cdot\text{d}/\text{m}^3$, gain k_{SRT} is in $^{\circ}\text{C}/\text{d}$, and gains k_{Tair} and $k_{Tsludge}$ are in $^{\circ}\text{C}/^{\circ}\text{C}$.

To properly compare the influence of each input, plant models (Equations (A1)–(A4)) were scaled. The scaling considered the equilibrium operating-points (Table 2) and the admissible excursion of the following variables: SRT from 10 d to 15 d, Qa from 1000 m^3/d to 65,000 m^3/d , and T_{air} and T_{sludge} from 10 $^{\circ}\text{C}$ to 20 $^{\circ}\text{C}$. Figure A1 depicts the magnitude frequency response ($s = j\omega$) [30] of the scaled plants. P_{Qa} magnitude is greater than P_{SRT} magnitude over the whole frequency band $\omega = [0, \infty]$ rad/d, which reveals that Qa is more powerful than SRT . Thus, plant P_{Qa} was planned to work at high frequencies to achieve better transient performance. P_{SRT} worked at the low frequency band. Controllers C_{Qa} and C_{SRT} handled the distribution of the working frequency band.

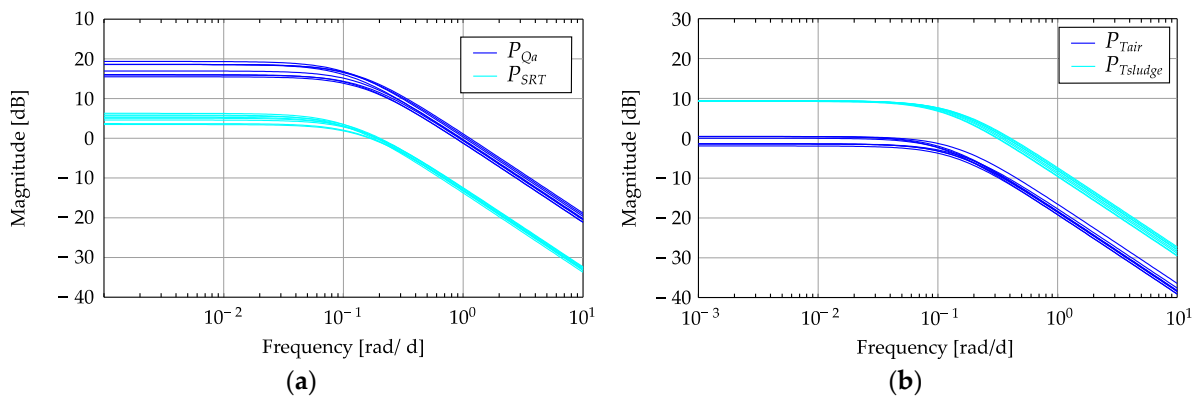


Figure A1. Scaled plant frequency responses.

Thanks to the contribution of the fast input (Qa), the steady state was reached more quickly at the output (T_{avg}) than at the slowest input (SRT). A maximum period of 20 days was chosen for SRT to reach its steady-state. Thus, $\omega = 0.2$ rad/d was chosen as the switching frequency for each branch participation.

The following frequency response model, $W_d(s = j\omega)$, expresses an upper limit for the desired frequency response T_{avg} when input step disturbances appear at T_{air} or T_{sludge} .

$$W_d(s)|_{s=j\omega} = \frac{1.621s}{(1+s)^2} \Big|_{s=j\omega} \quad (A5)$$

As stated in Section 2.2, $T_{avg}(t)$ must not deviate more than ± 0.6 $^{\circ}\text{C}$ from its set-point $T_{avg,ref}(t)$ whenever step changes of ± 5 $^{\circ}\text{C}$ take place at $T_{air}(t)$ or $T_{sludge}(t)$. Additionally, the set-point must be recovered no longer than seven days after the disturbance occurs (a temperature deviation inside a band of ± 0.05 $^{\circ}\text{C}$ around the set-point was assumed as recovered equilibrium). This dynamic performance was relatively ambitious for the sampling time $t_{s2} = 1$ d. Thus, the controllers were designed in the discrete domain using the z-transform [30], which makes the most of the available frequency band $\omega = [0, \pi/t_{s2}]$ rad/d. Note that the sampling time t_{s2} was in consonance with the discrete nature of the reactor operation: manipulated inputs Qa and SRT held during a 1-day batch, and

then a mean temperature T_{avg} was computed for the batch. Consequently, the equivalent of continuous plants (Equations (A1)–(A4)) into discrete plants yielded $P_{Qa}^{zoh}(z)$, $P_{SRT}^{zoh}(z)$, $P_{Tair}^{zoh}(z)$, $P_{Tsludge}^{zoh}(z)$. To achieve robust controllers, the required performance was an upper limit that must be observed by the whole set of plants [31]. This was formulated as:

$$\left| \frac{T_{avg}(z)}{T_{air}(z)} \right|_{z=e^{j\omega}} = \left| \frac{P_{Tair}^{zoh}(z)}{1 + P_{Qa}^{zoh}(z)C_{Qa}(z) + P_{SRT}^{zoh}(z)C_{SRT}(z)} \right|_{z=e^{j\omega}} \leq |W_d(j\omega)| \tag{A6}$$

and

$$\left| \frac{T_{avg}(z)}{T_{sludge}(z)} \right|_{z=e^{j\omega}} = \left| \frac{P_{Tsludge}^{zoh}(z)}{1 + P_{Qa}^{zoh}(z)C_{Qa}(z) + P_{SRT}^{zoh}(z)C_{SRT}(z)} \right|_{z=e^{j\omega}} \leq |W_d(j\omega)| \tag{A7}$$

A minimum phase margin of 45° was stated for robust stability despite uncorrelated variations of $P_{Qa}^{zoh}(z)$ and $P_{SRT}^{zoh}(z)$. This was formulated as:

$$\left| T_{Qa}(z) \right|_{z=e^{j\omega}} = \left| \frac{P_{Qa}^{zoh}(z)C_{Qa}(z)}{1 + P_{Qa}^{zoh}(z)C_{Qa}(z) + P_{SRT}^{zoh}(z)C_{SRT}(z)} \right|_{z=e^{j\omega}} \leq 1.3 \tag{A8}$$

$$\left| T_{SRT}(z) \right|_{z=e^{j\omega}} = \left| \frac{P_{SRT}^{zoh}(z)C_{SRT}(z)}{1 + P_{Qa}^{zoh}(z)C_{Qa}(z) + P_{SRT}^{zoh}(z)C_{SRT}(z)} \right|_{z=e^{j\omega}} \leq 1.3 \tag{A9}$$

Control specifications (Equations (A6)–(A9)) must be met for all discrete-equivalent plants and over the frequencies $\omega = [0, \pi]$ rad/d. Furthermore, the desired frequency band allocation was

$$\begin{aligned} \left| \frac{P_{SRT}^{zoh}(z)C_{SRT}(z)}{1 + P_{Qa}^{zoh}(z)C_{Qa}(z) + P_{SRT}^{zoh}(z)C_{SRT}(z)} \right|_{z=e^{j\omega}} &>> \left| \frac{P_{Qa}^{zoh}(z)C_{Qa}(z)}{1 + P_{Qa}^{zoh}(z)C_{Qa}(z) + P_{SRT}^{zoh}(z)C_{SRT}(z)} \right|_{z=e^{j\omega}}, \omega \in [0, 0.2] \\ \left| \frac{P_{Qa}^{zoh}(z)C_{Qa}(z)}{1 + P_{Qa}^{zoh}(z)C_{Qa}(z) + P_{SRT}^{zoh}(z)C_{SRT}(z)} \right|_{z=e^{j\omega}} &>> \left| \frac{P_{SRT}^{zoh}(z)C_{SRT}(z)}{1 + P_{Qa}^{zoh}(z)C_{Qa}(z) + P_{SRT}^{zoh}(z)C_{SRT}(z)} \right|_{z=e^{j\omega}}, \omega \in [0.2, \pi] \end{aligned} \tag{A10}$$

The controllers were designed via loop-shaping in the frequency domain to achieve the robust specifications (Equations (A6)–(A9)) with the participation of two control branches (Equation (A10)). Figure A2 shows how the shaping of the open-loop functions meet the bounds that represent the robust control specifications. A thorough description of the general methodology can be found in Rico-Azagra et al. [24]. The yielded controllers are Equations (3) and (4). Figure A3 proves the fulfilment of the robust control specifications (Equations (A6)–(A9)) and Figure A4 shows the frequency band allocation between branches (Equation (A10)).

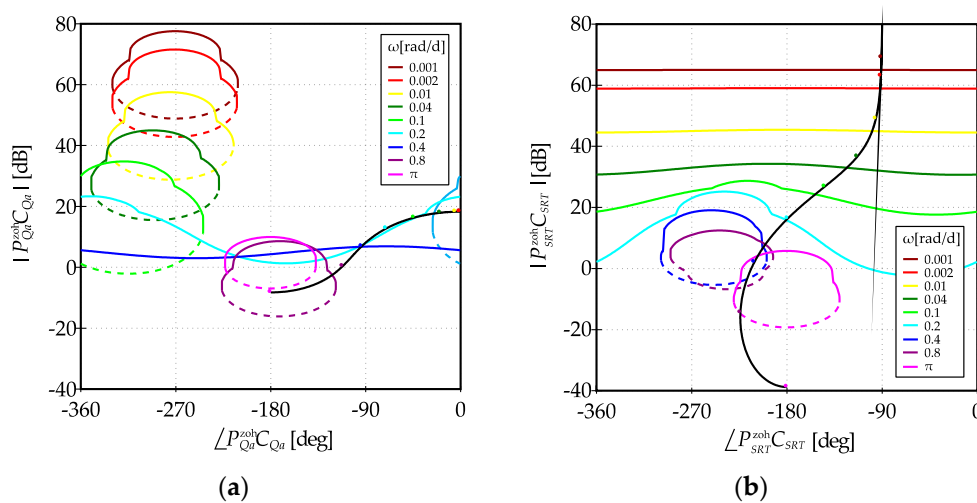


Figure A2. Loopshaping: (a) $P_{Qa}^{zoh}(z) C_{SRT}(z) C_{Qa}(z)$; and (b) $P_{SRT}^{zoh}(z) C_{SRT}(z)$.

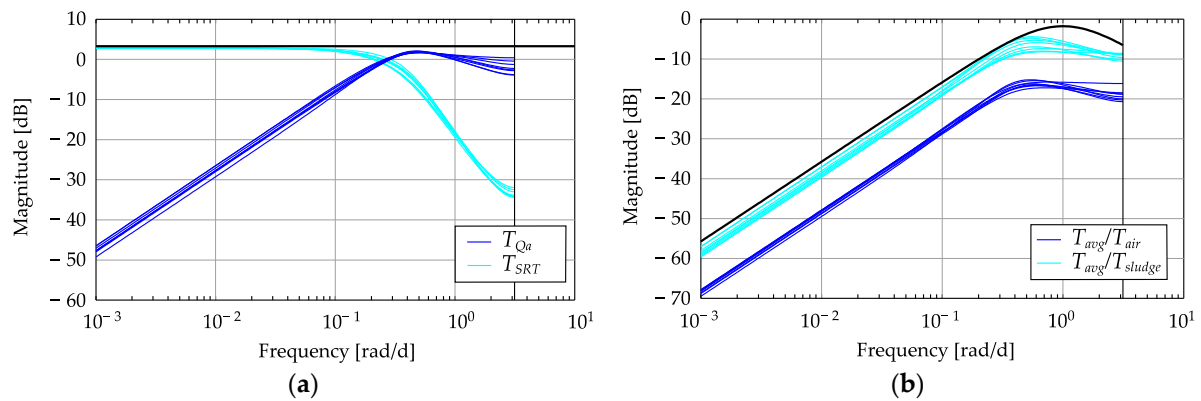


Figure A3. Specifications and closed-loop frequency responses: (a) stability; and (b) disturbance rejection.

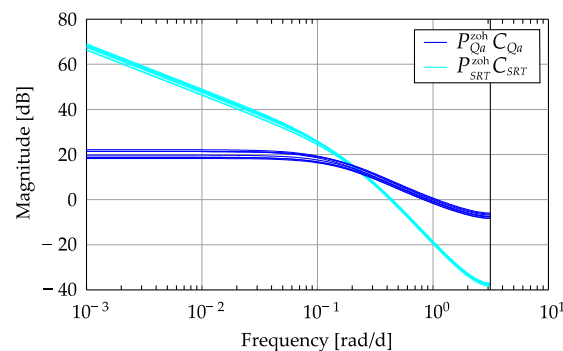


Figure A4. Frequency band distribution.

References

- Giffin, T. ATAD Process for the Treatment of Biosolids for Beneficial Re-Use. In Proceedings of the 72nd Annual Water Industry Engineers and Operators Conference, Bendigo Exhibition Centre, Bendigo, Australia, 1–3 September 2009.
- Lapara, T.M.; Alleman, J.E. Thermophilic aerobic biological wastewater treatment. *Water Res.* **1999**, *33*, 895–908. [[CrossRef](#)]
- Staton, K.L.; Alleman, J.E.; Pressley, R.L.; Eloff, J. 2nd Generation Autothermal Thermophilic Aerobic Digestion: Conceptual Issues and Process Advancements. In Proceedings of the WEF/AWWA/CWEA Joint Residuals and Biosolids Management Conference, San Diego, CA, USA, 21–24 February 2001.
- U.S. Environmental Protection Agency (USEPA). *Environmental Regulations and Technology: Control of Pathogens and Vector Attraction in Sewage Sludge*; EPA/625/R-92/013; U.S. Environmental Protection Agency, Office of Research and Development: Washington, DC, USA, 1992.
- Layden, N.M. An evaluation of autothermal thermophilic aerobic digestion (ATAD) of municipal sludge in Ireland. *J. Environ. Eng. Sci.* **2007**, *6*, 19–29. [[CrossRef](#)]
- Trim, B.C. Sludge Stabilization and Disinfection by means of Autothermal Aerobic Digestion using Oxygen. In Proceedings of the IWPC Biennial Conference, Durban, South Africa, 27–30 May 1984.
- Piterina, A.V.; Bartlett, J.; Pembroke, T.J. Evaluation of the Removal of Indicator Bacteria from Domestic Sludge Processed by Autothermal Thermophilic Aerobic Digestion (ATAD). *Int. J. Environ. Res. Public Health* **2010**, *7*, 3422–3441. [[CrossRef](#)] [[PubMed](#)]
- U.S. Environmental Protection Agency (USEPA). *Environmental Regulations and Technology: Autothermal Thermophilic Aerobic Digestion of Municipal Wastewater Sludge*; Technical Report; EPA/625/10-90/007; U.S. Environmental Protection Agency, Office of Research and Development: Washington, DC, USA, 1990.
- European Commission. *Working Document on Sludge—3rd Draft*; ENVE.3/LM; European Union Commission: Brussels, Belgium, 27 April 2000.

10. Breider, E.J.; Drnevich, R.F. Control of Sludge Temperature in Autothermal Sludge Digestion. U.S. Patent 4,276,174, 30 June 1981.
11. Kim, Y.K.; Oh, B.K. Aeration Control of Thermophilic Aerobic Digestion Using Fluorescence Monitoring. *J. Microbiol. Biotechnol.* **2009**, *19*, 93–98. [[PubMed](#)]
12. Wareham, D.G.; Mavinic, D.S.; Hall, K.J. Sludge Digestion Using ORP-Regulated Aerobic-Anoxic Cycles. *Water Res.* **1994**, *28*, 373–384. [[CrossRef](#)]
13. Zambrano, J.A. Autothermal Thermophilic Aerobic Digestion: Design of Controllers and Benchmarking Validation. Ph.D. Thesis, Universidad de Navarra, San Sebastian, Spain, 2011.
14. Nájera, S.; Zambrano, J.A.; Gil-Martínez, M. Improvements in ATAD using Quantitative Feedback Control and Nonlinear Generator of Optimal Operating Points. *Chem. Eng. Sci.* **2013**, *102*, 613–621. [[CrossRef](#)]
15. García, J.; Gomez, J.; Lasheras, A.; Huete, E.; Echeverría, N.; García-Heras, J.L. Advancing with ATAD. *Water Sci. Technol.* **2007**, *19*, 48–55.
16. Nájera, S.; Gil-Martínez, M.; Zambrano, J. ATAD control goals through the analysis of process variables and evaluation of quality, production and cost. *Water Sci. Technol.* **2015**, *71*, 717–724. [[CrossRef](#)] [[PubMed](#)]
17. Scisson, J.P. ATAD, the Next Generation: Design, construction, start-up and operation of the first municipal 2nd generation ATAD. In Proceedings of the WEF/AWWA/CWEA Joint Residuals and Biosolids Management Conference and Exhibition, Baltimore, MD, USA, 19–22 February 2003.
18. Velut, S.; de Mare, L.; Hagander, P. Bioreactor control using a probing feeding strategy and mid-ranging control. *Control Eng. Pract.* **2007**, *15*, 135–147. [[CrossRef](#)]
19. Haugwitz, S.; Hagander, P.; Norén, T. Modeling and control of a novel heat exchange reactor, the open plate reactor. *Control Eng. Pract.* **2007**, *15*, 779–792. [[CrossRef](#)]
20. Prado-Rubio, O.; Jörgensen, S.; Jonsson, G. pH control structure design for a periodically operated membrane separation process. *Comp. Chem. Eng.* **2012**, *43*, 120–129. [[CrossRef](#)]
21. Johnsson, O.; Sahlin, D.; Linde, J.; Lidén, G.; Hägglund, T. A mid-ranging control strategy for non-stationary processes and its application to dissolved oxygen control in a bioprocess. *Control Eng. Pract.* **2015**, *42*, 89–94. [[CrossRef](#)]
22. Alferes, J.; Irizar, I. Combination of extremum-seeking algorithms with effective hydraulic handling of equalization tanks to control anaerobic digesters. *Water Sci. Technol.* **2010**, *61*, 2825–2834. [[CrossRef](#)] [[PubMed](#)]
23. Houpis, C.H.; Rasmussen, S.J.; García-Sanz, M. *Quantitative Feedback Theory, Fundamentals and Applications*; Taylor and Francis: Boca Raton, FL, USA, 2006.
24. Rico-Azagra, J.; Gil-Martínez, M.; Elso, J. Quantitative Feedback Control of Multiple Input Single Output Systems. *Math. Probl. Eng.* **2014**, *2014*, 1–17. [[CrossRef](#)]
25. Zambrano, J.A.; Gil-Martínez, M.; García-Sanz, M.; Irizar, I. Benchmarking of control strategies for ATAD technology: A first approach to the automatic control of sludge treatment systems. *Water Sci. Technol.* **2009**, *60*, 409–417. [[CrossRef](#)] [[PubMed](#)]
26. Jeppsson, U.; Pons, M.N.; Nopens, I.; Alex, J.; Coop, J.B.; Gernaey, K.V.; Rosen, C.; Steyer, J.P.; Vanrolleghem, P. Benchmark simulation model no 2: General protocol and exploratory case studies. *Water Sci. Technol.* **2007**, *56*, 67–78. [[CrossRef](#)] [[PubMed](#)]
27. Gómez, J.; de Gracia, M.; Ayesa, E.; Garcia-Heras, J.L. Mathematical modelling of autothermal thermophilic aerobic digesters. *Water Res.* **2007**, *41*, 959–968. [[CrossRef](#)] [[PubMed](#)]
28. Vrecko, D.; Gernaey, K.V.; Rosen, C.; Jeppsson, U. Benchmark Simulation Model N° 2 in Matlab-Simulink: Towards plant-wide WWTP control strategy evaluation. *Water Sci. Technol.* **2006**, *54*, 65–72. [[CrossRef](#)]
29. Fuchs, L.; Fuchs, M. Process for the Disinfection and Aerobic Stabilization of Sewage Sludge; U.S. Patent 4,983,298, 8 January 1991.
30. Dorf, R.C.; Bishop, R.H. *Modern Control System*, 12th ed.; Pearson Prentice Hall: Upper Saddle River, NJ, USA, 2011.
31. Yaniv, O. *Quantitative Feedback Design of Linear and Nonlinear Control Systems*; Kluwer Academic Publishers: Norwell, MA, USA, 1999.

